Steel and Composite Structures, Vol. 6, No. 1 (2006) 55-69

DOI: http://dx.doi.org/10.12989/scs.2006.6.1.055

Experimental study on partially concrete-filled steel tubular columns

T. Ishizawa†, T. Nakano‡ and M. Iura‡†

Department of Civil and Environmental Engineering, Tokyo Denki University, Hatoyama, Hiki, Saitama, Japan

(Received March 4, 2005, Accepted July 26, 2005)

Abstract. The results of tests conducted on 11 concrete-filled steel tubular columns were reported. Concrete was partially filled in circular steel tubular columns. The primary test parameters were radius and thickness of steel tubes, concrete height, loading patterns and attachment of diaphragm and studs. Concrete strain was measured directly by embedding strain gauges so that the effect of diaphragm on concrete confinement could be investigated. The effects of concrete height and diaphragm on ultimate strength and ductility of steel tubes were investigated. The comparisons of the test results with the existing results for rectangular cross-sections were made on the basis of ultimate strength and ductility of concrete-filled steel tubular columns.

Key words: composite columns (concrete and steel); ductility; inelastic buckling; cyclic loading; PCFST columns.

1. Introduction

Great damage to steel bridge piers had been observed during the 1995 Kobe Earthquake in Japan. Although serious cracks have been observed in the existing steel piers, the main failure mode was local buckling of steel plates. The Public Works Research Institute *et al.* (1997) have published a series of reports for experimental works on bridge piers. Other research institutes in Japan have also conducted experimental and numerical works on steel bridge piers. In order to strengthen the existing steel bridge piers, various methods have been proposed. Important issues for retrofitting the existing steel bridge piers were strength and ductility. When the ultimate strength of a steel bridge pier increases, massive substructures will be required. Since reinforcement of the existing substructures is expensive and time consuming, the increase in ultimate strength is not desirable. On the other hand, the increase of ductility in steel bridge piers is favorable for seismic design. Longitudinal stiffeners (Iura *et al.* 1997), concrete infill (Iura *et al.* 2002, Usami and Ge 1994, Ge and Usami 1996), carbon fiber sheets (Watanabe *et al.* 2002) and patch plates (Chu *et al.* 2004) have been used to increase the ductility of steel piers. From an economic and construction point of view, concrete infill would be one of the best choices for increasing ductility.

†Research Assistant
‡Graduate Student
‡†Professor, Corresponding author, Email: iura@g.dendai.ac.jp

Concrete-filled steel tubular (CFST) columns have been used in many structural applications. Fam *et al*. (2004), Han *et al*. (2001), Inai *et al*. (2004), Murata *et al*. (2000), Varma *et al*. (2002) and Varma *et al*. (2004) have conducted experimental works on CFST columns subjected to axial compression and lateral loads. Kilpatrick and Rangan (1999) have investigated the effect of load eccentricities producing double curvature bending upon the behavior of CFST columns. Uy (2000) and Mursi and Uy (2003) have presented both an experimental and theoretical treatment of coupled local and global buckling of CFST columns. When concrete is fully filled in steel bridge piers, the strength and ductility of CFST columns increase. However, the increases in ultimate strength and dead load require massive substructures. Especially when the existing structures are retrofitted, the increases in ultimate strength and dead load are unfavorable for substructures. Therefore, partially concrete-filled steel tubular (PCFST) columns have received wide attention in steel bridge piers. Amano *et al.* (1998) have proposed an optimum concrete volume for rectangular PCFST columns. Ge and Usami (1996) have reported experimental results for rectangular cross-sections and shown that the attachment of a diaphragm on the top of concrete increases the ultimate strength and ductility of rectangular PCFST columns. Susantha *et al.* (2002) have proposed a numerical model of rectangular CFST columns subjected to cyclic loading. According to Usami and Ge (1994), the filled-in concrete prevented steel plates from buckling inside columns. Therefore, the ultimate strength of rectangular PCFST columns increases.

In comparison with works comcerning rectangular PCFST columns, a small number of studies have been reported on circular ones. According to Iura *et al*. (1997), an elephant foot bulge was a typical local buckling mode of circular columns. In this case, steel plates deformed outside columns, so that the filled-in concrete did not prevent steel plates from buckling. Iura *et al*. (1998) have developed the formulae for evaluating ultimate strength and optimum concrete volume for circular PCFST columns. Morishita *et al*. (2000) have shown that attachment of a diaphragm on the top of concrete increases ultimate strength and ductility of circular PCFST columns. The specimens used in Morihsita *et al.* (2000) have the small radius-to-thickness (r/t) ratio of 23. Hu *et al*. (2003) have pointed out that confining pressures on CFT columns subjected to axial compression are affected by the r/t ratio. Therefore, test results for large r/t ratios are indispensable for understanding the mechanical behavior of circular PCFST columns.

In this paper, experimental results for 11 PCFST columns and 1 hollow column with circular cross-sections are reported. Test parameters are radius and thickness of steel tubes, concrete strength, concrete height, loading patterns and attachment of a diaphragm and studs. The specimens have r/t ratios ranging from 35 to 59 and concrete strengths ranging from 22 to 37 MPa. In order to investigate confinement effects by diaphragm, concrete strain gauges are embedded in 4 test specimens.

2. Test setup

It is seldom feasible to model a complete structure due to technical and economic difficulties. The height of test specimens was determined on the basis of the present testing system, as shown in Fig. 1. The specimen was built in at one end, and was subjected to axial and lateral loads at the other end. The axial load corresponds to the dead load transmitted from girders onto bridge piers. The lateral load corresponds to the earthquake load. The jack for the axial load is movable along a guide rail so that the direction of the axial load remains unchanged during the test. The convex plate was placed between the jack and the test specimen so that the top of the specimen was allowed to rotate. The axial compression

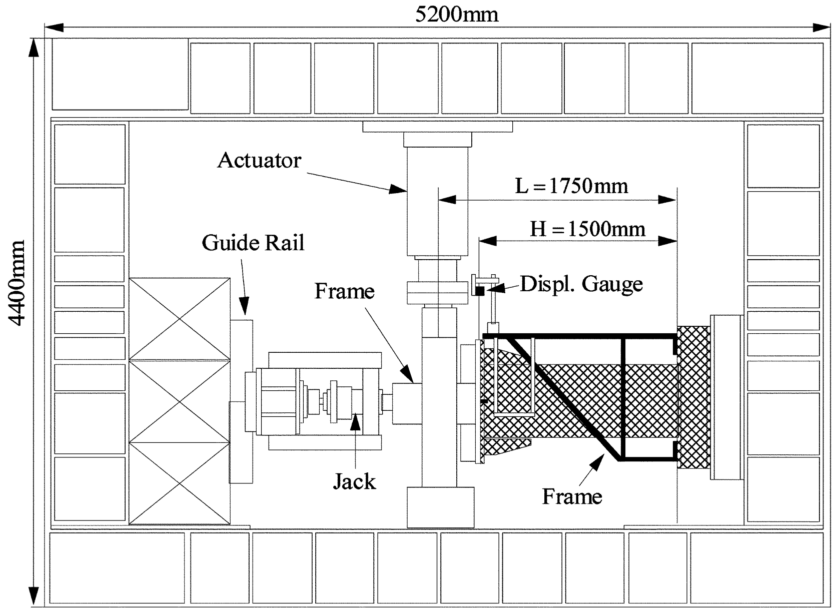

Fig. 1 Test setup

load was applied and maintained constant during the test. The lateral load was applied using the hydraulic actuator under displacement control. A displacement gauge was set up at the top of the specimen, as shown in Fig. 1.

3. Test specimens and loading conditions

A typical specimen in the test is shown in Fig. 2. The geometry and material properties of test specimens are shown in Table 1, in which R is the radius of tube, t the thickness of steel plate, l_c the height of concrete and l_d the position of diaphragm. The definition of l_c and l_d is given in Fig. 2. The diaphragm has an inside hole with radius $r_0 = R/2$, as shown in Fig. 2, so that concrete is easily filled

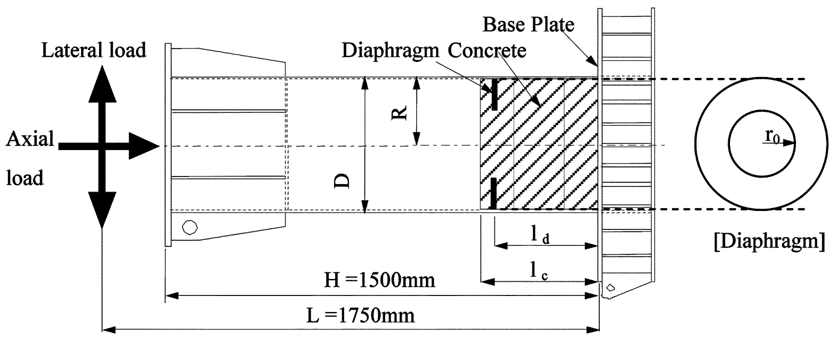

Fig. 2 Test specimen

Table 1 Geometry and material properties of test specimens

Specimen	R	t	l_c	γ	l_d	σ_y	σ_c	σ_t	Loading Condition
	mm	mm	mm	%	mm	MPa	MPa	MPa	
No.1	255	4.35	-	-	-	288	-	-	1 cycle
No.2	251	5.76	160	9	-	287	22.4	2.21	1 cycle
No.3	251	5.76	300	17	-	287	22.4	2.21	1 cycle
No.4	251	5.94	998	57	-	270	36.3	2.96	1 cycle
No.5	250	5.76	998	57	-	313	37.1	3.12	1 cycle
No.6	250	5.76	998	57	988	313	37.1	3.12	1 cycle
No.7	250	5.76	998	57	stud	313	37.1	3.12	1 cycle
No.8	251	5.94	998	57	-	270	36.3	2.96	monotone
No.9	250	5.76	998	57	998	313	37.1	3.12	monotone
No.10	200	5.77	600	34	600	312	22.6	1.69	1 cycle
No.11	200	5.78	600	34	400	287	26.0	2.08	1 cycle
No.12	200	5.77	600	34	-	312	22.6	1.69	1 cycle

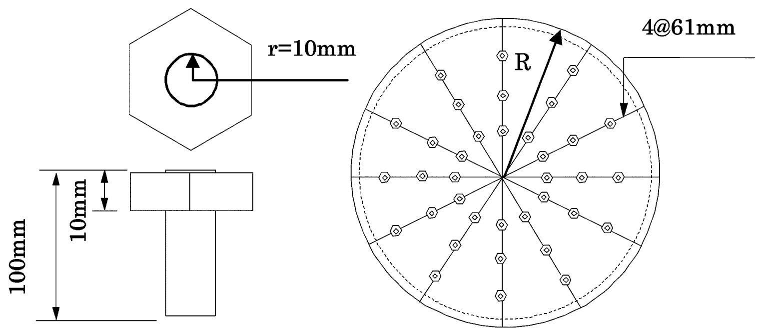

Fig. 3 Detail of stud

into the test specimen. Since specimen No.1 is a hollow tube, the blanks of specimen No.1 in Table 1 show that neither concrete nor diaphragm exists. The blanks of specimens No.2 to No.5, No.8 and No.12 denote that no diaphragm exists. The notation "stud" in specimen No.7 denotes that 36 studs are placed at the bottom of the steel tube, as shown in Fig. 3. The notation γ in Table 1 denotes the ratio of concrete and steel tube height, defined as

$$\gamma = l_c / 1750 \times 100(\%) \tag{1}$$

Steel plates of the test specimens were made of JIS SS400. Coupons from steel plates were tested. The lower yield stress of steel σ_y, the concrete compression strength σ_c and the concrete tension strength σ_t are shown in Table 1.

Two types of loading patterns were employed in this test. The first type was a monotonous loading and the second one was a quasi-statically cyclic loading. The cyclic loading program consisted of one cycle at an absolute displacement magnitude of $\pm\delta_y$, of $\pm 2\delta_y$,…., until the specimen failed or the hydraulic actuator reached its limit. The magnitude δ_y denotes the lateral displacement, in which the displacement gauge is placed, and is determined so that the bottom surface of the test specimen reaches

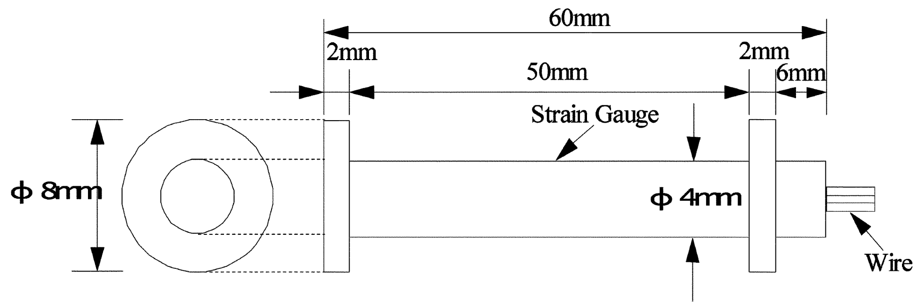

Fig. 4 Detail of concrete strain gauge

a yield stress. The explicit expression for δ_y is obtained by introducing x=L–H into the result of Timoshenko and Goodier (1970), and expressed as

$$\delta_y = \frac{P_y H^3}{3EI} + \frac{P_y H^2 (L-H)}{2EI} + \frac{P_y H}{\kappa G A} \tag{2}$$

where

$$P_y = \frac{(\sigma_y - N/A) I}{LR} \tag{3}$$

in which E, G, I, A denote Young's modulus, shear modulus, moment inertia and cross-section area of the steel tube, respectively, $\kappa = 2/3$ and the other notations are shown in Fig. 2. The last term in Eq. (2) shows the effect of shear deformation on the tip displacement. The magnitude of axial load was determined so that axial stress was 15% of yield stress of steel plate.

Concrete strain gauges, as shown in Fig. 4, were embedded in specimens No.4, 7 to 9 in order to measure concrete strains. The strain gauge was water-repellent and placed between two flanges. The concrete strain gauges were embedded at fixed points near steel plates by using a prop.

4. Experimental results

4.1. Position of steel local buckling

The failure mode of the present tests resulted in elephant foot bulge or local inelastic buckling of steel plates. The position of steel local buckling is shown in Fig. 5. Black half circles, denoted by B, show the position of steel local buckling. The notations D and S, as shown in Fig. 5, denote diaphragms and studs, respectively. An arrow above the test specimen expresses the loading direction; test specimens No.1 to No.7 and No.10 to No.12 were subjected to cyclic lateral loading, while test specimens No.8 and No.9 were subjected to monotonous lateral loading. The positions of steel local buckling may be classified into the following three cases:

a) Local buckling occurred at the bottom of column (No.1, No.3 to No.10 and No.12)

b) Local buckling occurred on the top of concrete (No.2)

c) Local buckling occurred above diaphragm (No.11).

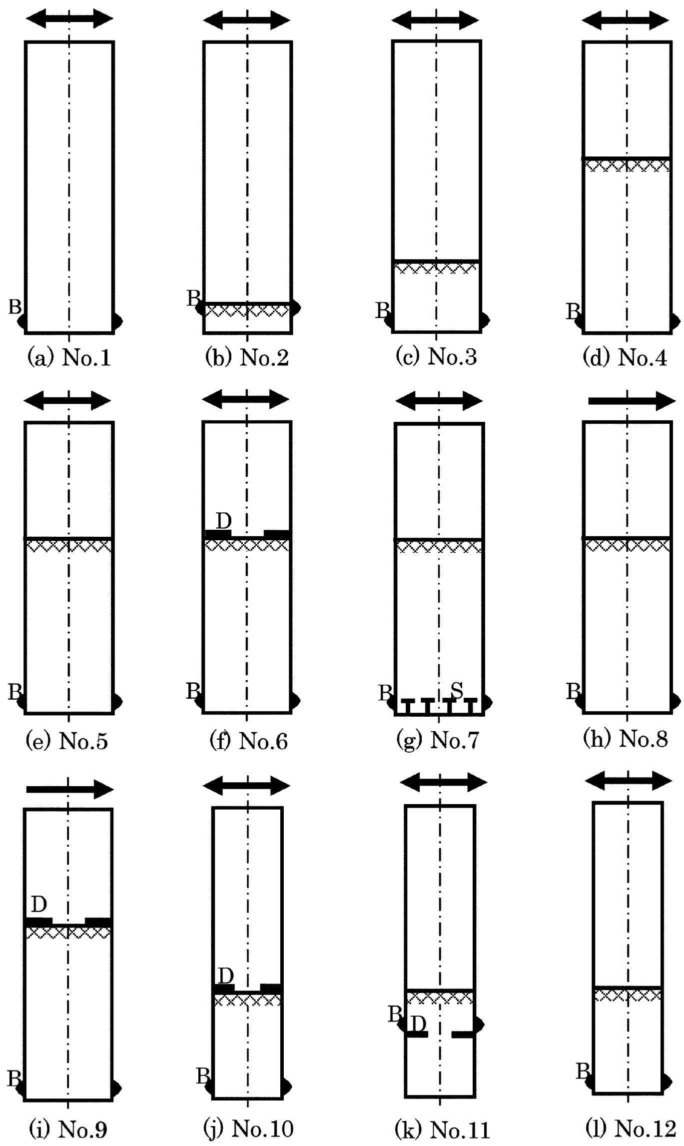

Fig. 5 Failure modes of PCFST columns

When the concrete height was low (e.g., specimen No.2), local buckling occurred on the top of concrete. A similar buckling pattern was observed among the damaged bridge piers during the 1995 Kobe Earthquake. The bases of existing steel bridge piers have been strengthened by partially filling in concrete for protecting the piers from automobile collision. Since the height of concrete filled into the existing steel bridge piers was low, the local buckling was observed on the top of concrete. When the concrete height increased (e.g., specimens No.3 to No.5), local buckling occurred at the bottom of the column. When a diaphragm was embedded in concrete (e.g., specimen No.11), local buckling occurred above the diaphragm.

4.2. Hysteretic curves

Hysteretic curves for lateral load and tip displacement of test specimens are shown in Fig. 6. The hysteretic curve for No.1, in which concrete is not filled, is shown in Fig. 6(a). The hysteretic curves

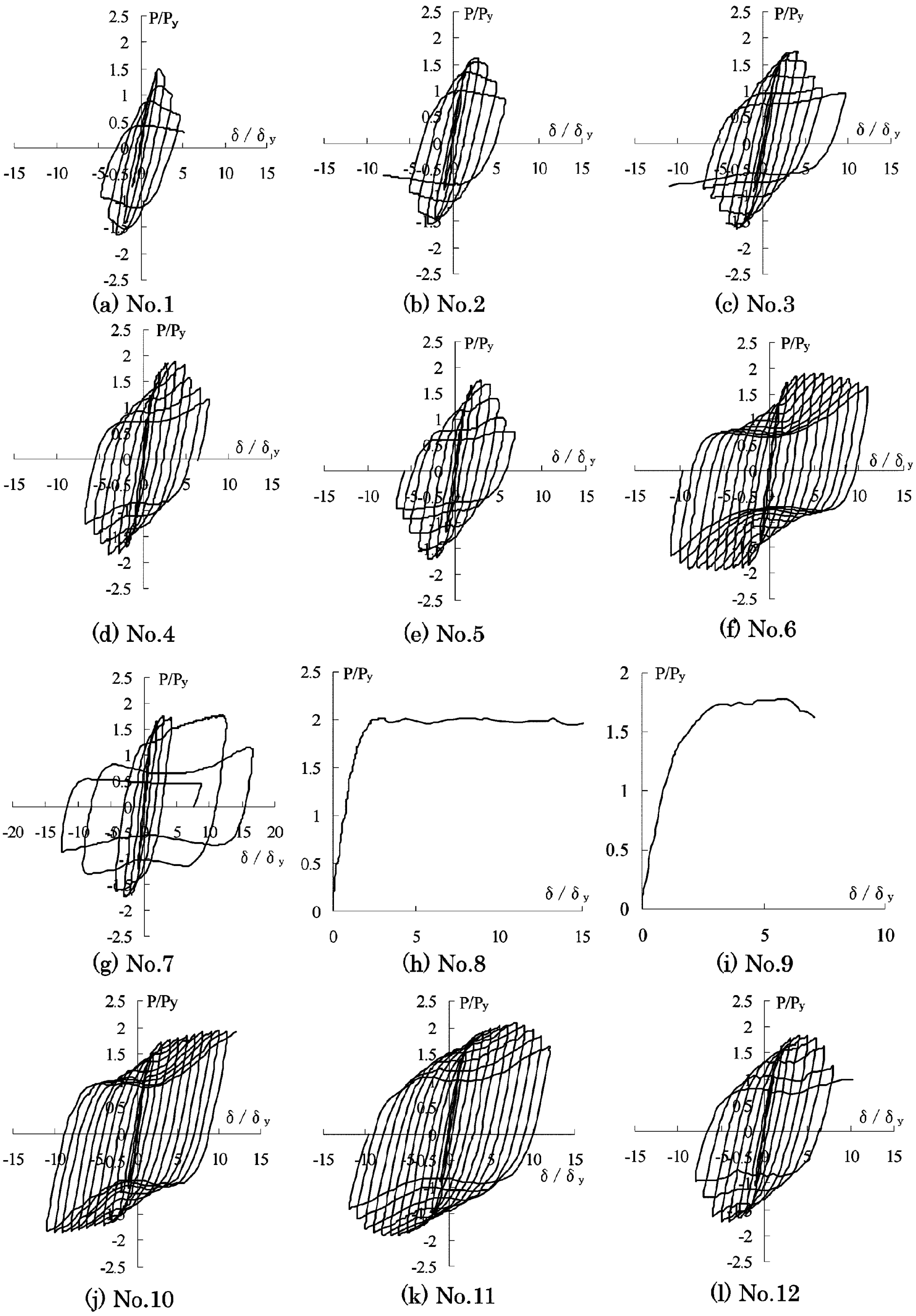

Fig. 6 Hysteretic curves

may be influenced by concrete height, position of diaphragm, an existence of studs and loading pattern. These effects on hysteretic curves will be discussed in the following.

4.2.1. Effect of concrete height

The specimens No.2, 3 and 4 were tested to investigate the effects of concrete height on ductility and maximum load of PCFST columns. The hysteretic curve of No.2, in which local buckling occurred on the top of concrete, is shown in Fig. 6(b). Note that the hysteretic curve of No.2 is similar to that of No.1, in which high ductility was not obtained. In both cases, the maximum loads were observed in the third loading cycle. After the column reached its maximum load, the load-carrying capacity decreased drastically. Hysteretic curves of specimens No.3 and 4, in which local buckling occurred at the bottom of column, are shown in Figs. 6(c) and 6(d), respectively. The maximum loads in No.3 and No.4 were observed in the fourth and fifth loading cycles, respectively. The ductility of No.3 and No.4 was relatively higher than that of No.2. A difference between specimens No.3 and No.4 was found in concrete strength in addition to concrete height. The concrete strength and height of specimen No.4 were about 1.6 and 3 times higher than those of specimen No.3, respectively. In spite of this fact, the ductility of specimen No.4 did not increase substantially compared with that of specimen No.3.

A difference in hysteretic curves between specimens No.2 and No.4 is found in the curves after the maximum loads. In the case of specimen No.4, a hardening was observed after the fifth loading cycle, while a hardening was not observed in specimen No.2. A question may arise whether or not the hardening continues if the applied displacement increases in specimen No.4. In order to investigate the hardening effect on the hysteretic curve, a special loading pattern was employed in specimen No.5. Before local buckling of steel plates occurred, a conventional cyclic loading was employed. After the local buckling occurred, the applied displacement increased until decrease on the load was observed. The hysteretic curve of specimen No.5 is shown in Fig. 6(e). No significant difference in the hysteretic curves between specimens No.4 and No.5 was observed. It is worth noting that the load-carrying capacity does not increase even if the loading pattern is changed.

4.2.2. Effect of diaphragm and studs

In the case of specimen No.6, a diaphragm was attached on the top of concrete. The specimen size and concrete height of specimen No.6 were the same as those of specimens No.4 and No.5. The hysteretic curve of specimen No.6 is shown in Fig. 6(f). Steel local buckling occurred at the fourth loading cycle. Even after the local buckling occurred, the load-carrying capacity of specimen No.6 did not decrease and high ductility was obtained. The maximum load of specimen No.6 was 9% higher than that of specimen No.5. Therefore the attachment of a diaphragm plays an important role for increasing ductility without increasing maximum load.

Since a diaphragm would be welded before filling concrete, an operation for filling concrete should be done in a narrow space. Therefore we considered the use of studs instead of a diaphragm. Welding studs is a conventional task, and a large operation space will be available for filling concrete. As shown in Fig. 3, in the case of specimen No.7, 36 studs were attached at the bottom of the column. The loading pattern of specimen No.7 was the same as that of specimen No.5; after local buckling occurred, the applied displacement increased until decrease on the load was observed. The hysteretic curve of specimen No.7 is shown in Fig. 6(g), in which high ductility is observed while the maximum load is almost the same as that of specimen No.5. The attachment of studs might prevent a separation between concrete and base plate, so that a high ductility was obtained.

4.2.3. Effect of loading pattern

A monotonic loading pattern was employed in specimens No.8 and No.9. The geometry of specimens No.8 and No.9 is the same as that for No.5 and No.6, respectively. The hysteretic curves of specimens No.8 and No.9 are shown in Figs. 6(h) and 6(i), respectively. In the case of specimen No.9, the test terminated due to the crack on the welding between the base plate and the column. The deficiency in welding might have led to the crack. If the base plate and the column were welded adequately, a high ductility would be obtained. The reason for showing the test results of specimen No.9 is that concrete strain gauges are embedded to investigate mechanical behavior of concrete, which will be discussed later.

A comparison between Figs. 6(e) and 6(h) shows that monotonic loading leads to a higher ductility than cyclic loading. In the case of cyclic loading, concrete was subjected to both compression and tension. After a few cycles, the concrete suffered great damage due to the tensile forces. Therefore the load-carrying capacity of PCFST columns decreases. In the case of monotonic loading, on the other hand, the steel plate and concrete act on tension and compression sides of PCFST columns, respectively. Therefore high ductility was obtained under monotonic loading.

4.2.4. Specimen with small radius

The radius of specimens No.1 to No.9 was about 250mm, while the radius of specimens No.10 to No.12 was about 200 mm. The height of all of specimens used was 1500mm. The radius-to-thickness ratio of specimens No.10 to No.12 was 35. The specimens No.10 to No.12 had the same geometry except for a diaphragm. A diaphragm was attached on the top of concrete of specimen No.10, and it was attached in the concrete of specimen No.11. Specimen No.12 had no diaphragm. The concrete strength of these specimens was smaller than those of specimens No.4 to No.9.

The hysteretic curves of specimens No.10 to No.12 are shown in Figs. 6(j) to 6(l), respectively. As expected, high ductility was obtained in specimen No.10, in which a diaphragm was attached on the top of concrete. Although the maximum load of specimen No.11 was higher than others, the load-carrying capacity decreased after the maximum load. This is because steel local buckling of specimen No.11 occurred above the diaphragm. Comparison between Figs. 6(j), (k) and (l) shows that a diaphragm attached on the top of concrete plays an important role to increase ductility.

The hysteretic curve of specimen No.10, as shown in Fig. 6(j), is similar to that of specimen No.6, as shown in Fig. 6(f). In both specimens, a diaphragm was attached on the top of concrete. Although concrete strengths were different, high ductility was obtained in both specimens.

4.3. Strain gauges in concrete

Hu *et al.* (2003) have studied the influence of the concrete confining pressure of columns on the uniaxial behavior of CFST columns. It was found that good confining effects to concrete were obtained especially when the radius to thickness ratio is small (say r/t<20). Ricles and Paboojian (1994) have demonstrated the significance of concrete confinement on the cyclic behavior of composite columns. According to Furlong (1967), in the case of CFST columns, no increase in concrete strength due to confinement by steel tubes was observed. As far as PCFST columns are concerned, the attachment of a diaphragm increases the ductility of columns. The confinement pressures by the diaphragm may lead to high ductility. In order to investigate the confinement effects directly, we measured the concrete strains by embedding the concrete strain gauge, as shown in Fig. 4.

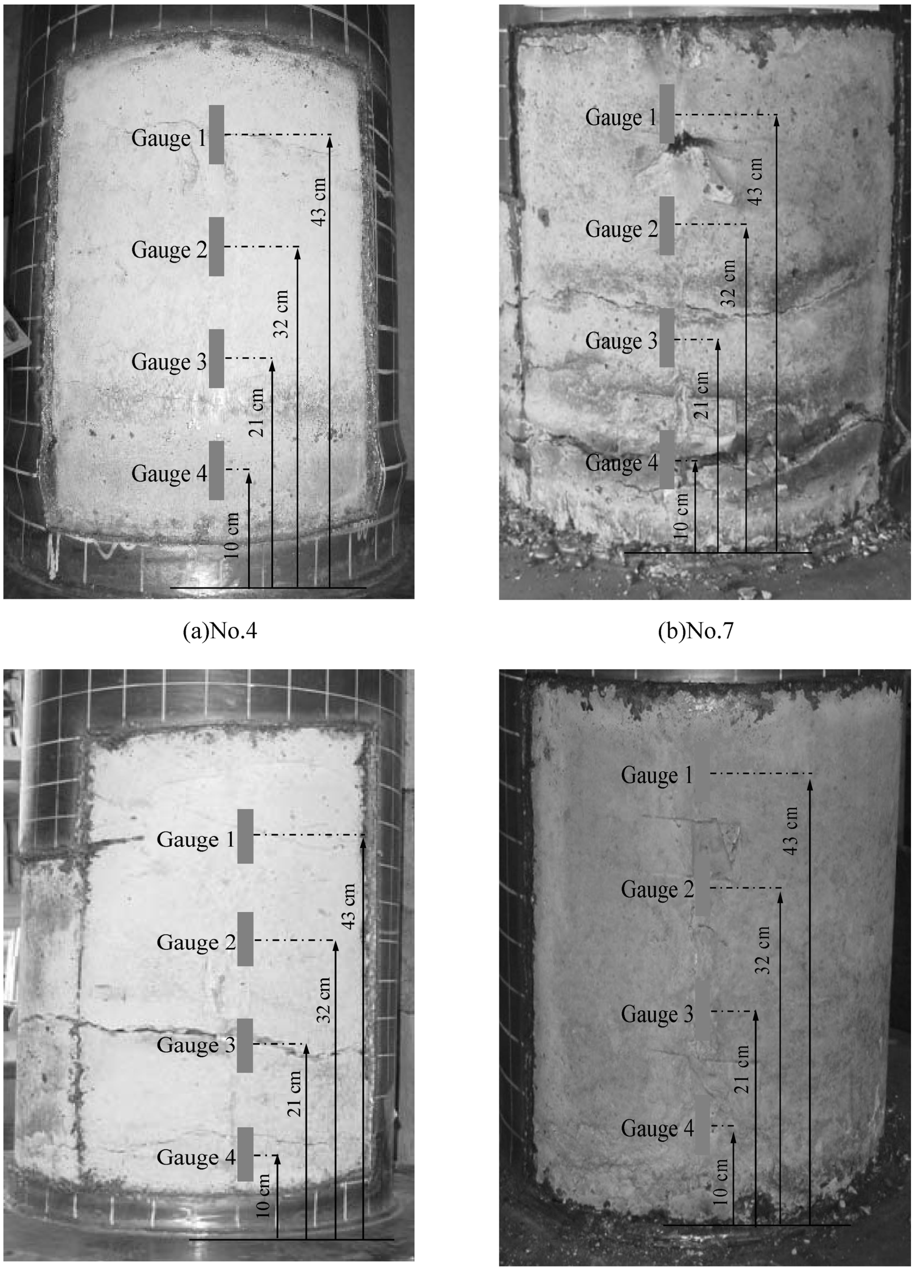

(a)No.4 (b)No.7

(c)No.8 (d)No.9

Fig. 7 Positions of concrete strain gauges

In order to investigate the mechanical behavior of concrete, concrete strain gauges were embedded in specimens No.4, No.7, No.8 and No.9. According to Table 1, the concrete strength of all the specimens was about 37 MPa. Cyclic loading was applied to specimens No.4 and No.7, while monotonic loading was applied to specimens No.8 and No.9. Specimen No.9 had a diaphragm, and specimen No.7 had studs. Both specimens No.4 and No.8 had no diaphragm. The positions of concrete strain gauges are shown in Fig. 7, in which concrete after the test is shown. As shown in Fig. 7, the distance from gauge 1, gauge 2, gauge 3 and gauge 4 to the base plate was 43 cm, 32 cm, 21 cm and 10 cm, respectively. The relationships between loads and concrete strains are shown in Fig. 8. It is shown in Fig. 8 that the load-strain curves change their directions drastically at a specific load. In order to investigate this phenomenon, we picked-up specimen No.8. As shown in Fig. 7(c), a vivid crack formed on the gauge 3. The load-strain curves are shown in Fig. 8(c). It is shown that the strain in gauge 3 takes infinite value just before 81 kN, and that other strains change their directions at 81 kN. Therefore this load is defined as the concrete crack initiation load, which is shown in Fig. 8 as dotted lines. In the case of specimens No.4 and No.7, concrete crack initiation loads are defined as loads where the load-strain curves change their directions. In the case of specimen No.9, the strain in gauge 2 takes infinite value before other strains change their directions. This fact shows that a crack might occur around gauge 2. In this case, therefore, the concrete crack initiation load is defined when the infinite strain is obtained.

In the case of specimens No.4 and No.8, which had no diaphragm, the concrete crack initiation loads were 67 kN and 81 kN, respectively. In the case of specimens No.7 and No.9, which had a

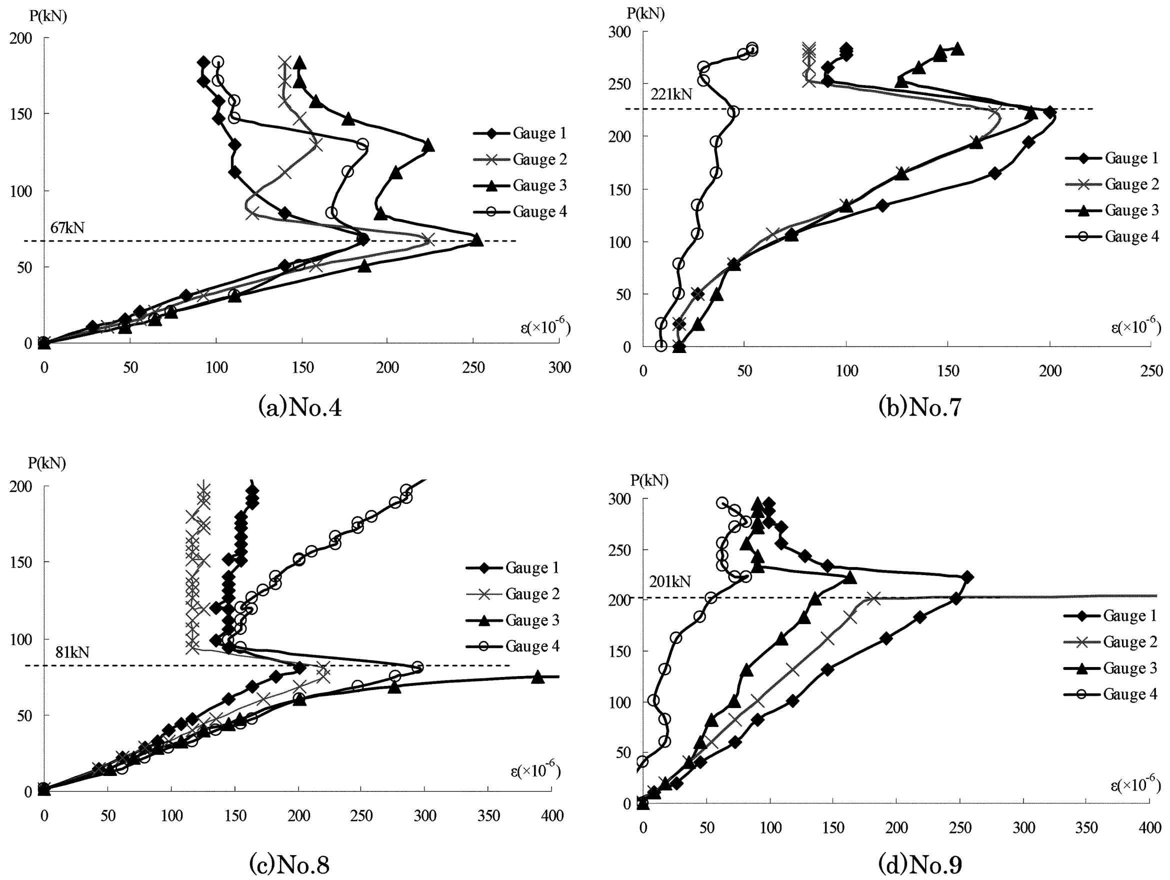

Fig. 8 Concrete crack initiation loads

diaphragm, the concrete crack initiation loads were 221 kN and 201 kN, respectively. These results show that the concrete crack initiation load increases substantially with attachment of diaphragm on the top of concrete. In other words, attachment of diaphragm provides the confining pressure to the concrete.

5. Discussions

It is important to discuss the difference in mechanical behavior of columns between circular cross-sections and rectangular ones. For comparison, we employed the experimental results for rectangular cross-sections conducted by Ge and Usami (1996).

First, the effects of concrete volume on maximum load and ductility are discussed. The specimens used for comparison have no diaphragm. The number of experimental results used is three for rectangular PCFST columns and five for circular ones. The relationships between maximum load and concrete volume are shown in Fig. 9(a). The maximum loads of rectangular PCFST columns do not increase with the increase of concrete volume. For circular PCFST columns, the maximum loads increase slightly with the increase of concrete height.

The ductility is defined herein as the ratio δ_{max}/δ_y, where δ_{max} denotes the tip displacement at the maximum load and δ_y is defined by Eq. (2). The relationships between ductility and concrete volume are shown in Fig. 9(b). The ductility increases with the increase of concrete volume in both rectangular and circular PCFST columns.

Second, we investigated the effects of diaphragm and studs on maximum load and ductility. The test specimens used for comparison have the same geometry except for a diaphragm or studs. Four experimental results were used for rectangular columns, while six were used for circular PCFST columns. The effect of diaphragm on maximum load is shown in Fig. 10(a), in which P^{w}_{max} and P^{n}_{max} denote the maximum loads of columns with and without a diaphragms or studs, respectively. For rectangular PCFST columns, the increase of maximum loads was up to 22%. For circular PCFST columns, when a diaphragm was attached on the top of concrete, the increase of maximum loads was up to 9%. When a diaphragm was embedded in concrete (specimen No.11), increase of maximum loads was 13%. Note that a decrease of maximum loads is found in specimen No.7 with studs. As far

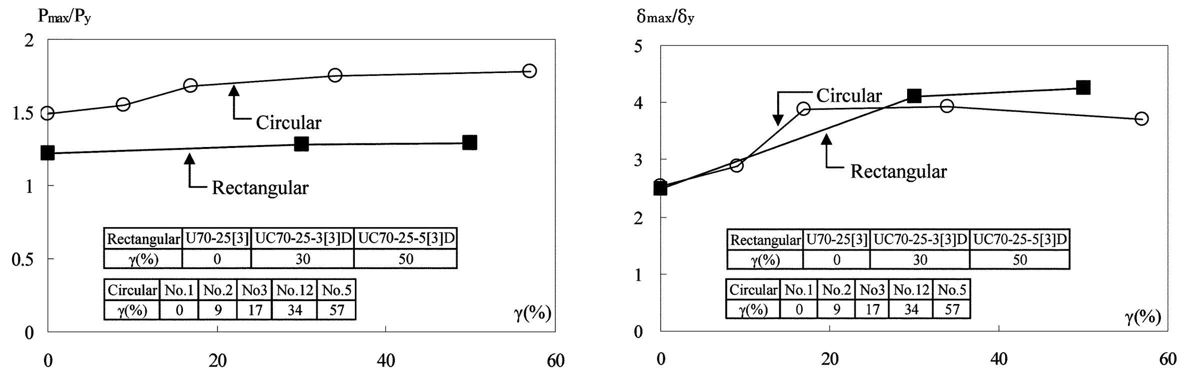

(a)Maximum load (b)Ductility

Fig. 9 Effects of concrete volume on maximum loads and ductility

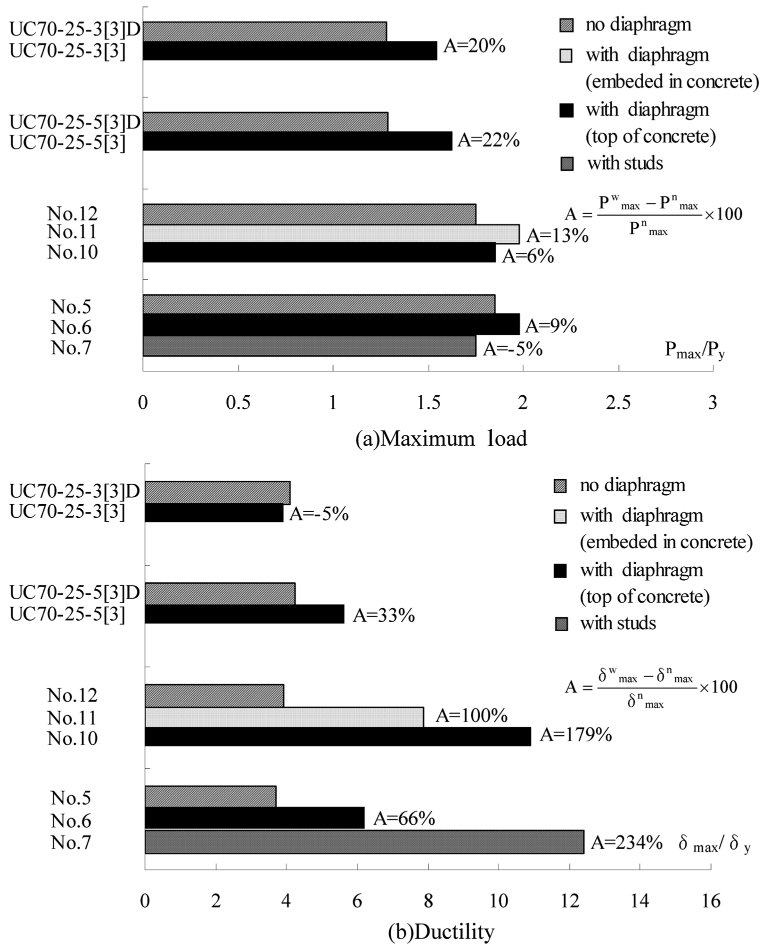

Fig. 10 Effects of diaphragm on maximum loads and ductility

as the maximum load is concerned, attachment of diaphragm is more effective in rectangular PCFST columns rather than circular ones.

The effect of diaphragm or studs on ductility is shown in Fig. 10(b), in which $\delta^w_{\max}$ and $\delta^n_{\max}$ denote the displacements at maximum load of columns with and without a diaphragm or studs, respectively. For rectangular PCFST columns, a small decrease for ductility was observed between specimens UC70-25-3[3]D and UC70-25-3[3], while a 33% increase was observed between specimens UC70-25-5[3]D and UC70-25-5[3]. For circular PCFST columns, a 179% increase was observed between specimens No.12 and No.10, and a 66% increase between specimens No.5 and No.6. When a diaphragm was embedded in concrete (specimen No.11), the increase of ductility was 100%. In the case of specimen No.7 with studs, the increase of ductility is 234%.

It is shown from Fig. 10 that attachment of diaphragms or studs is very effective for circular PCFST columns because high ductility and low increase of maximum load are obtained.

6. Conclusions

The behavior of PCFST columns was experimentally investigated. The effects of concrete volume, diaphragm and studs on maximum strength and ductility of PCFST columns were studied. The following observations and conclusions were made on the basis of the present experimental results:

a) The position of steel local buckling depended on concrete volume and the position of diaphragm. When concrete volume was small, steel local buckling occurred on the top of concrete.
b) A hardening was observed in the hysteretic curves when concrete volume increased. However, high ductility would not be obtained without the use of a diaphragm.
c) High ductility can be obtained, when concrete is filled enough and a diaphragm is attached on the top of concrete.
d) Maximum load of circular PCFST columns increased slightly by attaching diaphragm.
e) Attachment of studs at the bottom of PCFST columns led to a significant increase in ductility and a low increase in maximum load.
f) Attachment of diaphragm or studs delayed the concrete crack initiation and increased the concrete confining pressure.

Acknowledgements

This work has been supported by the Research Institute for Science and Technology at Tokyo Denki University.

References

Amano, M., Kasai, A., Usami, T., Ge, H., Okamoto, S. and Maeno, H. (1998), "Experimental and analytical study on elasto-plastic behavior of partially concrete-filled steel piers", *J. Struct. Eng.*, JSCE, **44A**, 179-188.

Chu, K. and Sakurai, T. (2004), "Reinforcement method for improvement of earthquake-proof capacity on existing cylindrical steel piers by welded steel plates", *The 2nd Int. Conf. on Steel & Composite Structures*, Seoul, Korea, September 2-4.

Fam, A., Qie, F.S. and Riakalla, S. (2004), "Concrete-filled steel tubes subjected to axial compression and lateral cyclic loads", *J. Struct. Eng.*, ASCE, **130**(4), 631-640.

Furlong, R.E. (1967), "Strength of steel-encased concrete beam-columns", *J. Struct. Eng.*, ASCE, **93**(5), 113-125.

Ge, H. and Usami, T. (1996), "Cyclic tests of concrete-filled steel box columns", *J. Struct. Eng.*, ASCE, **122**(10), 1169-1177.

Han, L.H., Zhao, X.L. and Tao, Z. (2001), "Tests and mechanics model for concrete-filled SHS stub columns, columns and beam-columns", *Steel and Composite Structures*, **1**(1), 51-74.

Hu, H.T., Huang, C.S., Wu, M.H. and Wu, Y.M. (2003), "Nonlinear analysis of axially loaded concrete-filled tube columns with confinement effect", *J. Struct. Eng.*, ASCE, **129**(10), 1322-1329.

Inai, E., Mukai, A., Kai, M., Tokinoya, H., Fukumoto, T. and Mori, K. (2004), "Behavior of concrete-filled steel tube beam column", *J. Struct. Eng.*, ASCE, **130**(2), 189-202.

Iura, M., Kumagai, Y. and Komaki, O. (1997), "Ultimate strength of stiffened cylindrical shells subjected to axial and lateral forces", *J. Struct. Mech. and Earthq. Eng.*, JSCE, No.556/I-38, 107-118.

Iura, M., Kumagai, Y. and Komaki, O. (1998), "Strength and ductility of cylindrical steel piers subjected to cyclic lateral load", *J. Struct. Mech. and Earthq. Eng.*, JSCE, No.598/I-44, 125-135.

Iura, M., Orino, A. and Ishizawa, T. (2002), "Elasto-plastic behavior of concrete-filled steel tubular columns", *J. Struct. Mech. and Earthq. Eng.*, JSCE, No.696/I-58: 285-298.

Kilpatrick, A.E. and Rangan, B.V. (1999), "Tests on high-strength concrete-filled steel tubular columns", *ACI Struct. J.*, **96**(2), 268-274.

Morishita, M., Aoki, T. and Suzuki, M. (2000), "Experimental study on the seismic resistance performance of concrete-filled steel tubular columns", *J. Struct. Eng.*, JSCE, **46A**, 73-83.

Murata, K., Yamada, M., Ikeda, M., Takiguchi, M., Watanabe, T. and Kinoshita, M. (2000), "Revaluation of ductility for concrete-filled tubular steel columns", *J. Struct. Mech. and Earthq. Eng.*, JSCE, No.640/I-50, 149-163.

Public Works Research Institute, Metropolitan Expressway Public Corp., Hanshin Expressway Public Corp., Nagoya Expressway Public Corp., Kozai Club, Japan Association of Steel Bridge Construction. (1997), *Joint Research Report on Limit State Seismic Design of highway Bridge Piers* (I-VII).

Ricles, J.M. and Paboojian, S.D. (1994), "Seismic performance of steel encased composite columns", *J. Struct. Eng.*, ASCE, **120**(8), 2474-2494.

Susantha, K.A.S., Ge, H. and Usami, T. (2002), "Cyclic analysis and capacity prediction of concrete-filled steel box columns", *Earthq. Eng. Struct. Eng.*, **31**. 195-216.

Timoshenko, S.P. and Goodier, J.N. (1970), *Theory of Elasticity*, 3rd edition, p.46.

Usami, T. and Ge, H. (1994), "Ductility of concrete-filled steel box columns under cyclic loading", *J. Struct. Eng.*, ASCE, **120**(7), 2021-2040.

Uy, B. (2000), "Strength of concrete filled steel box columns incorporating local buckling", *J. Struct. Eng.*, ASCE, **126**(3), 341-352.

Mursi, M. and Uy, B. (2003), "Strength of concrete filled steel box columns incorporating interaction buckling", *J. Struct. Eng.*, ASCE, **129**(5), 626-639.

Varma, A., Ricles, J.M., Sause, R. and Lu, L.W. (2002), "Experimental behavior of strength square concrete-filled steel tube beam-columns", *J. Struct. Eng.*, ASCE, **128**(3), 309-318.

Varma, A., Ricles, J.M., Sause, R. and Lu, L.W. (2004), "Seismic behavior and design of high-strength square concrete-filled steel tube beam columns", *J. Struct. Eng.*, ASCE, **130**(2), 169-179.

Watanabe, T., Ishida, K., Hayashi, K., Yamaguchi, T. and Ikeda. S. (2002), "Seismic retrofit of steel piers with carbon fiber sheets", *J. Struct. Eng.*, JSCE, **48A**, 725-734.

CC